

STRESS DISTRIBUTION AROUND DISCONTINUITIES IN SOFT ELASTIC MEMBRANES

Salvatore S. Ligarò and Paolo S. Valvo*

Department of Structural Engineering
University of Pisa, Pisa, Italy
e-mail: s.ligaro@ing.unipi.it, p.valvo@ing.unipi.it

Key words: Wrinkly Membranes, Non-linear Elasticity, Stress Concentration

Abstract. *The paper is concerned with the determination of the stress distribution in the regions of a soft elastic membrane surrounding geometrical or structural discontinuities, such as holes, slits, inclusions or local stiffeners. The severity of the stress concentration is assessed through a general non-linear model that considers large displacements, large deformations and a non-linear elastic material law. Inability of the membrane of sustaining any compressive stress, highlighted by the occurrence of wrinkling and local buckling, is automatically accounted for by recourse to the concept of relaxed strain energy. Solution of the stated problem is obtained within a FEM framework, where an arc-length path-tracing procedure allows to follow the evolution of the phenomenon. Applications present the case of a rectangular membrane endowed with a circular or straight central defect – a void or a rigid inclusion. Numerical results show that when wrinkling is taken into account the stress-concentration differs significantly from that predicted by the standard membrane theory, being in some cases less severe.*

1 Introduction

The study of the stress distributions in a soft elastic membrane constitutes a fundamental problem in bioengineering, chemistry and biology. At the same time, it is an attractive object of research in aircraft, spacecraft and civil engineering [1, 2].

The lack of bending stiffness characterises the behaviour of a real membrane, preventing it from sustaining compressive stresses of appreciable value, even when a remarkable extensional stiffness is exhibited under tension. Broadly speaking, loss of stability is referred to as *buckling* when the deformed configuration shows low-frequency undulations, and *wrinkling* when small-amplitude high-frequency waves materialise [3].

Experimenting on an initially flat elastic membrane subject to planar loads, we observe that three types of regions can be clearly individualised on its equilibrium configuration:

- a) *taut* or *active* regions, where both principal stresses are positive (tensile) or zero;
- b) *wrinkled* regions, where one principal stress is positive or zero and the other one is negative (compressive, although negligible in value);
- c) *slack* or *inactive* or *buckled* regions, where both principal stresses are negative (again negligible in value).

A major difficulty in treating equilibrium problems concerning a partly wrinkled membrane is that the boundaries of the aforesaid regions are *a priori* unknown. Moreover, if the membrane is made of a soft material, then these evolve continuously during the loading process. Consequently, one should also account for the possibility of large deformations and adopt a non-linear material law.

The problem considered in this paper appears under many respects even harder. In fact, our will to know led us to ask what effects would be produced by the introduction of geometric or structural discontinuities – such as holes, slits, local stiffeners or rigid inclusions – in an ideal membrane. In these cases, achieving some solutions, even approximate, requires a number of different phenomena to be taken simultaneously into account.

The model we propose here treats each stated issue through a specific tool. In particular:

- a) large deformations are considered by adopting the Green-Lagrange measure of strain;
- b) material non-linearity is entered by using Ogden's law [4];
- c) wrinkling and buckling phenomena are automatically accounted for by modifying the assumed constitutive law, according to Pipkin's concept of *relaxed energy* density [5, 6];
- d) the governing set of non-linear equilibrium equations is derived via the principle of stationary (minimum) total potential energy;
- e) solutions are obtained in a FEM context based on a total Lagrangian formulation;
- f) the evolution of the phenomenon is monitored via an incremental-iterative procedure of the arc-length type [7].

As a application, we present the cases of a rectangular membrane endowed with circular or straight central defects – voids or rigid inclusions. Results show that if wrinkling is considered, the stress-concentration changes significantly with respect to the standard membrane theory. This is qualitatively highlighted by the surfacing of different location and extension of taut, wrinkled and slack regions around the defect.

2 Problem formulation

2.1 Geometry

An initially flat membrane occupies in the unstressed reference configuration, C^* , the region Ω of the plane OXY , bounded by the curve Γ . The membrane thickness, h , is assumed to be constant and negligible with respect to the in-plane dimensions of the body. The displacement vector, $\mathbf{u} = \bar{\mathbf{u}}$, is prescribed on a part, Γ_u , of Γ . In-plane edge traction, $\mathbf{t} = \mu \bar{\mathbf{t}}$, proportional to a single multiplier, $\mu \in \mathcal{R}^+$, is assigned on the part Γ_p . On the boundary, Γ_i , surrounding the internal defect proper conditions will be posed each time.

Let $\mathbf{X} = [X, Y, 0]^T$ be the position vector of the material point, $P \in \Omega$, in the reference configuration. In a variable configuration, C , that point occupies a new position, $\mathbf{x} = [x, y, z]^T$, thus experiencing a total displacement, $\mathbf{U} = \mathbf{x} - \mathbf{X} = [u, v, w]^T$.

In a wrinkled region points experience small or moderate out-of-plane displacements, while the displacement gradient, $\partial\mathbf{U}/\partial\mathbf{X}$, shows high-frequency oscillations. Instead, in a buckled region out-of-plane displacements can be large. So, a suitable measure of strain is given by the Green-Lagrange tensor

$$\mathbf{E} = \frac{1}{2} \left[\left(\frac{\partial\mathbf{U}}{\partial\mathbf{X}} \right) + \left(\frac{\partial\mathbf{U}}{\partial\mathbf{X}} \right)^T + \left(\frac{\partial\mathbf{U}}{\partial\mathbf{X}} \right)^T \left(\frac{\partial\mathbf{U}}{\partial\mathbf{X}} \right) \right]. \quad (1)$$

Because of its thinness, at equilibrium the membrane can be considered to be in a prevailing state of generalised plane stress. So, the relevant strain components are E_{XX} , E_{YY} and $G_{XY} = 2E_{XY}$, since $E_{XZ} = E_{YZ} = 0$ and E_{ZZ} is a function of the remaining ones.

According to Wu [3], the strain vector, $\mathbf{e} = [E_{XX}, E_{YY}, G_{XY}]^T$, can be written out as

$$\mathbf{e} = \boldsymbol{\varepsilon} + \boldsymbol{\varepsilon}^w, \quad (2)$$

where the *planar strain vector*, $\boldsymbol{\varepsilon}$, accounts for the contribution of the components u and v , while the *wrinkle strain vector*, $\boldsymbol{\varepsilon}^w$, depends on the out-of-plane displacement, w .

2.2 Material non-linearity

We suppose the membrane to be made of a homogeneous isotropic hyper-elastic material of the type proposed by Ogden, whose energy density expressed in terms of the principal stretches, λ_1 , λ_2 , and λ_3 , is the function

$$\hat{\omega}(\lambda_1, \lambda_2, \lambda_3) = \sum_{p=1}^N \frac{\mu_p}{\alpha_p} (\lambda_1^{\alpha_p} + \lambda_2^{\alpha_p} + \lambda_3^{\alpha_p} - 3). \quad (3)$$

Limiting the above summation to $N = 3$ and adopting the hypothesis of incompressibility

$$\lambda_1 \lambda_2 \lambda_3 = 1, \quad (4)$$

one obtains the expression

$$\omega(\lambda_1, \lambda_2) = \sum_{p=1}^3 \frac{\mu_p}{\alpha_p} (\lambda_1^{\alpha_p} + \lambda_2^{\alpha_p} + (\lambda_1 \lambda_2)^{-\alpha_p} - 3). \quad (5)$$

From (5) we derive the expressions for Biot's principal stresses, t_1 and t_2 , which are work-conjugate to the principal stretches, λ_1 and λ_2

$$\begin{aligned} t_1 &= \frac{\partial \omega}{\partial \lambda_1} = \frac{1}{\lambda_1} \sum_{p=1}^3 \mu_p [\lambda_1^{\alpha_p} - (\lambda_1 \lambda_2)^{-\alpha_p}], \\ t_2 &= \frac{\partial \omega}{\partial \lambda_2} = \frac{1}{\lambda_2} \sum_{p=1}^3 \mu_p [\lambda_2^{\alpha_p} - (\lambda_1 \lambda_2)^{-\alpha_p}]. \end{aligned} \quad (6)$$

2.3 The relaxed energy

Depending on the values assumed by λ_1 and λ_2 , the principal stresses (6) may be positive or negative, in the latest case contradicting the stated inability of the membrane of sustaining compressive stresses. To obviate this inconsistency, the energy density function, ω , must be modified in such a way that compressive stresses within wrinkled and slack regions are inhibited.

According to Pipkin [5], this can be done replacing the function ω appearing in (5) with a *relaxed energy*, ω_{rel} . Based on the circumstance that any folding of the membrane surface must take place leaving unchanged its strain energy, ω_{rel} will depend on the planar strain vector, $\boldsymbol{\varepsilon}$, only, while the wrinkle strain vector, $\boldsymbol{\varepsilon}^w$, does not play any role in the following analysis.

Recognition of the different-in-type regions of a membrane surface is based on the concept of *natural width* [5]. We say that a point P belongs to a *taut* region, if the planar principal stretches, λ_1 and λ_2 , satisfy there the conditions

$$\lambda_1 \geq \lambda_2^{-1/2} \quad \text{and} \quad \lambda_2 \geq \lambda_1^{-1/2}. \quad (7)$$

Vice versa, point P belongs to a *wrinkled* region if

$$\lambda_1 > 1 \text{ and } 0 < \lambda_2 < \lambda_1^{-1/2}, \text{ or, alternatively, if } \lambda_2 > 1 \text{ and } 0 < \lambda_1 < \lambda_2^{-1/2}, \quad (8)$$

Finally, we consider point P belonging to an *inactive* (*slack* or *buckled*) region if

$$0 < \lambda_1 \leq 1 \text{ and } 0 < \lambda_2 \leq 1. \quad (9)$$

The *relaxed energy*, ω_{rel} , is then defined as follows

$$\omega_{rel}(\lambda_1, \lambda_2) = \begin{cases} 0, & 0 < \lambda_1 < 1 \text{ and } 0 < \lambda_2 < 1, \\ \omega(\lambda_1, \lambda_1^{-1/2}), & \lambda_1 \geq 1 \text{ and } 0 < \lambda_2 < \lambda_1^{-1/2}, \\ \omega(\lambda_2^{-1/2}, \lambda_2), & 0 < \lambda_1 < \lambda_2^{-1/2} \text{ and } \lambda_2 \geq 1, \\ \omega(\lambda_1, \lambda_2), & \lambda_1 \geq \lambda_2^{-1/2} \text{ and } \lambda_2 \geq \lambda_1^{-1/2}, \end{cases} \quad (10)$$

where ω is still given by (5). With this, local buckling and wrinkling phenomena are formally treated as a physical non-linearity.

2.4 Solution strategy

By adopting a total Lagrangian formulation, we define a modified total potential energy of the system as

$$\Pi(u, v, \mu) = \int_{V_0} \omega_{rel} dV - \mu \int_{\Gamma_p} \bar{\mathbf{t}} \cdot \mathbf{u} d\Gamma \quad (11)$$

where $\mathbf{u} = [u, v]^T$ denotes the planar displacement vector, while V_0 and Γ_p refer to the volume and the loaded boundary of the membrane in C^* , respectively.

For a given load parameter, μ , equilibrium of the system corresponds to stationary points for the functional (11). Then, solving the system of equilibrium equations for increasing values of the load multiplier, μ , permits the tracing of the equilibrium path, which fully describes the evolution of the phenomenon.

For the sake of brevity, details of the solution strategy are here omitted and will be postponed to a forthcoming paper.

3 Applications

Applications here presented are concerned with the analysis of an initially flat rectangular membrane endowed with a central discontinuity, circular or straight in shape. The membrane is $2B = 100\text{ mm}$ wide and $2L = 400\text{ mm}$ long. Its thickness is $h = 0.1\text{ mm}$. The defect has diameter $2a = 10\text{ mm}$ (Figure 1a). Edges parallel to the X -axis are constrained to remain straight and are subjected to an increasing load, $\mathbf{t} = \mu \bar{\mathbf{t}} = \mu [0, \bar{t}]^T$, where $\bar{t} = 0.02\text{ N/mm}$. Edges parallel to the Y -axis are traction-free.

The following values

$$\begin{aligned} \mu_1 = 0.63\text{ MPa}, \quad \mu_2 = 0.0012\text{ MPa}, \quad \mu_3 = -0.01\text{ MPa}, \\ \alpha_1 = 1.3, \quad \alpha_2 = 5.0, \quad \alpha_3 = -2.0, \end{aligned} \quad (13)$$

were used for Ogden's strain energy density function.

In presenting our results, we will refer to a *reference longitudinal stretch*, which is defined as

$$\lambda = \frac{L+v}{L}, \quad (12)$$

where $2v$ is the relative longitudinal displacement between the two transversal edges, and to a *reference stress* defined as

$$S_{YY}^{REF} = \frac{\mu}{\lambda} \frac{\bar{t}}{h}. \quad (12)$$

3.1 Rectangular membrane with a central circular hole

In the first case discussed, the membrane is endowed with a central circular hole (Figure 1a). Thanks to symmetry, only a quarter of the membrane needs to be considered in the FEM model. It comprises 557 nodes and 995 constant strain/constant stress triangular elements, including 20 "very stiff" elements that were used to enforce the rigidity constraint at the loaded edge (Figure 1b).

Analysis was carried out twice. First, the standard membrane theory was used, where both tensile and compressive stresses are allowed. Then, the wrinkled membrane theory described in the previous section was applied. Results of the two analysis cases are illustrated by means of Figures 2 through 4.

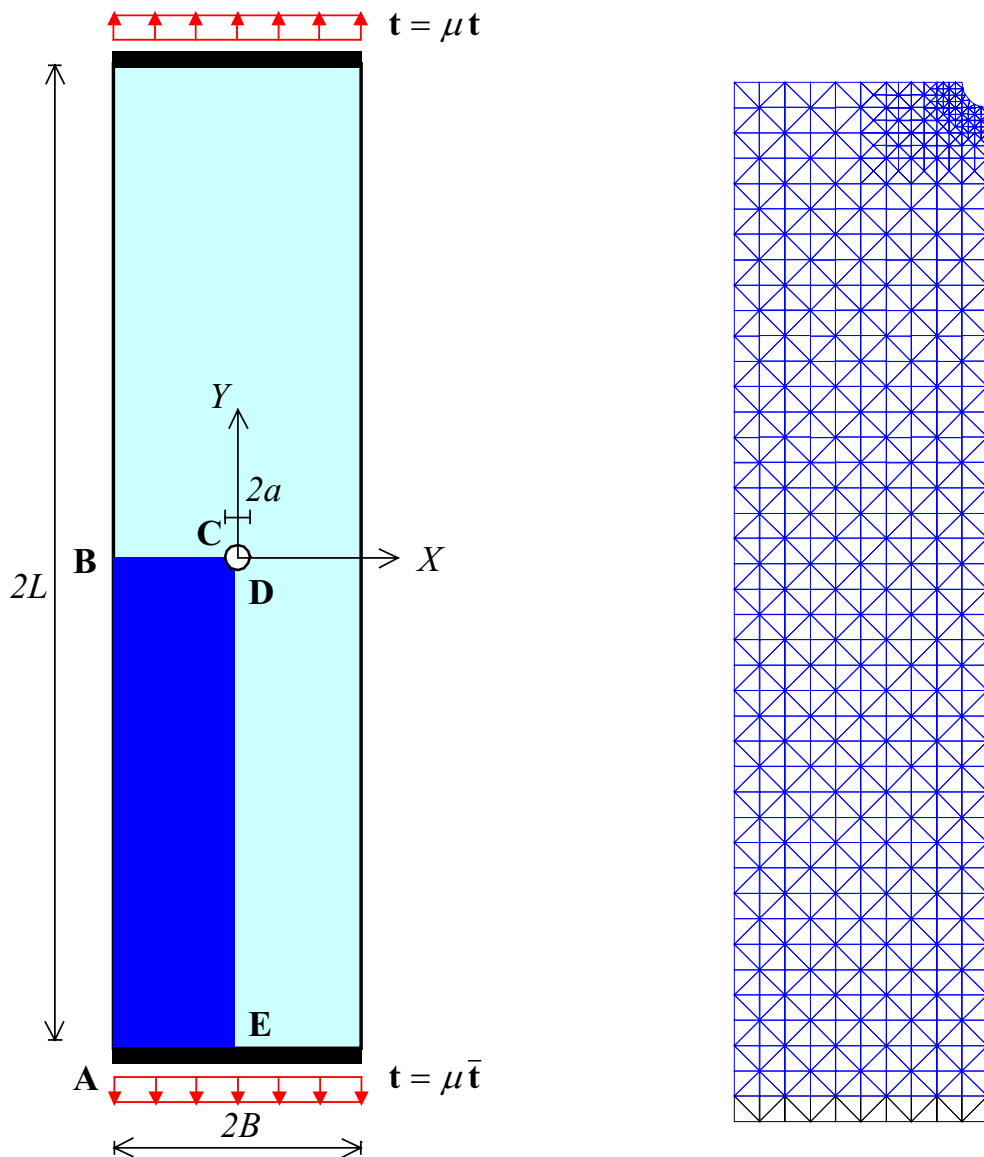


Figure 1: Rectangular membrane with a central circular defect: a) geometry and loads; b) FEM model.

Figure 2a represents the load multiplier, μ , as a function of the reference longitudinal stretch, λ . No appreciable discrepancy can be noticed between the two analysis cases, meaning that the global behaviour of the membrane is the same. Figures 2b, 2c and 2d show the transversal and longitudinal displacements of points **B**, **C** and **D** of the membrane as the load multiplier, μ , is increased. It is evident that larger displacements are obtained from the wrinkled membrane theory model, which results to have a lower stiffness.

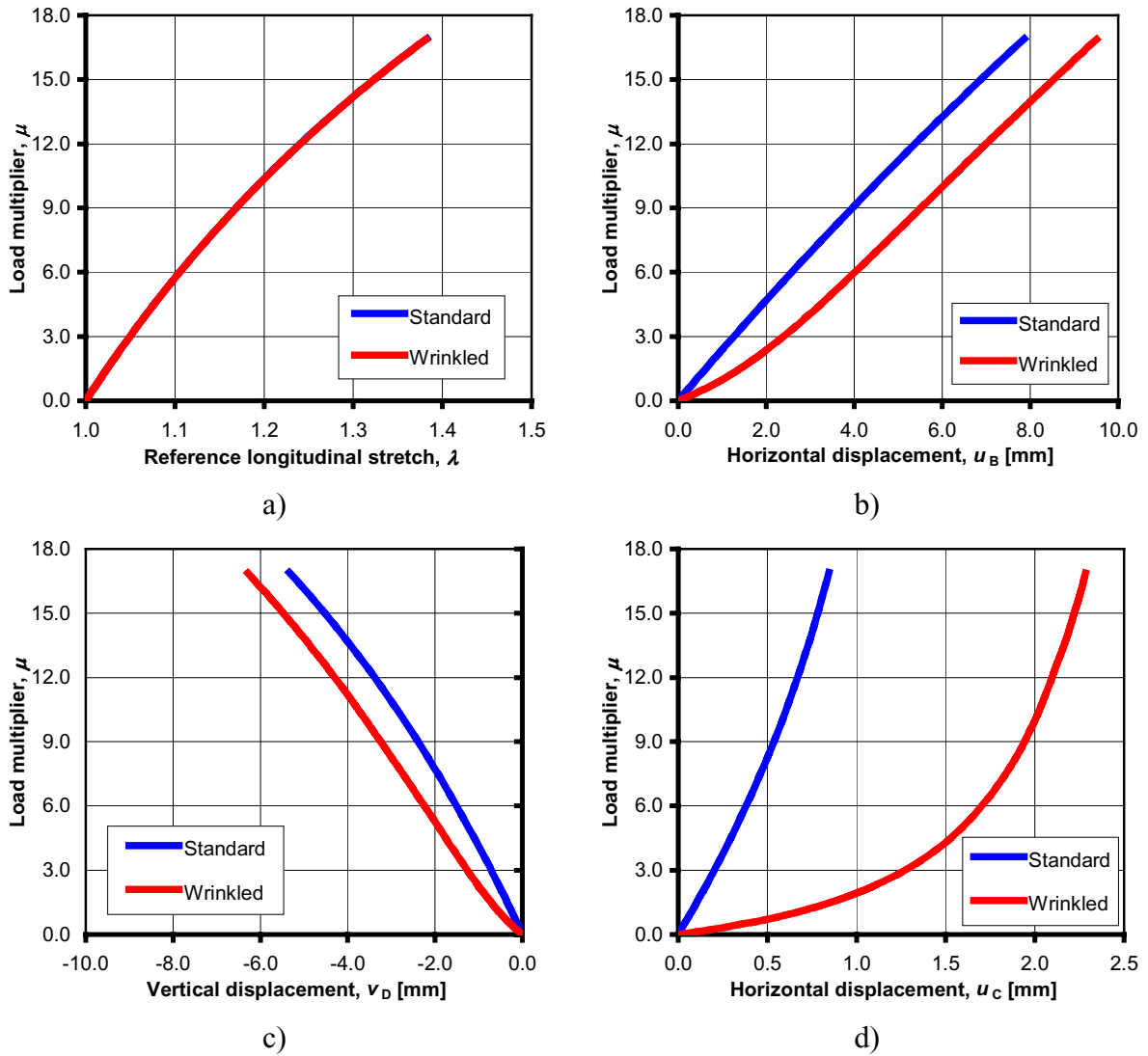


Figure 2: Rectangular membrane with a central circular hole: equilibrium path.

The stress-concentration around the geometrical discontinuity is different in the two analysis cases. Figure 3a shows the ratio, S_{XX}^C/S_{YY}^{REF} , between the X stress component in the neighbourhood of point C and the reference stress, as a function of the reference longitudinal stretch, λ . The S_{XX} stress-concentration appears to be less severe if wrinkling effects are considered.

The opposite is true for S_{YY} . This is evidenced by Figure 3b that represents the ratio, S_{YY}^C/S_{YY}^{REF} , between S_{YY} in the neighbourhood of C and S_{YY}^{REF} , as a function of λ . For both analysis cases, this stress-concentration tends to unity as the reference longitudinal stretch is increased. In fact, as the membrane experiences larger and larger displacements, it conforms to the applied loads.

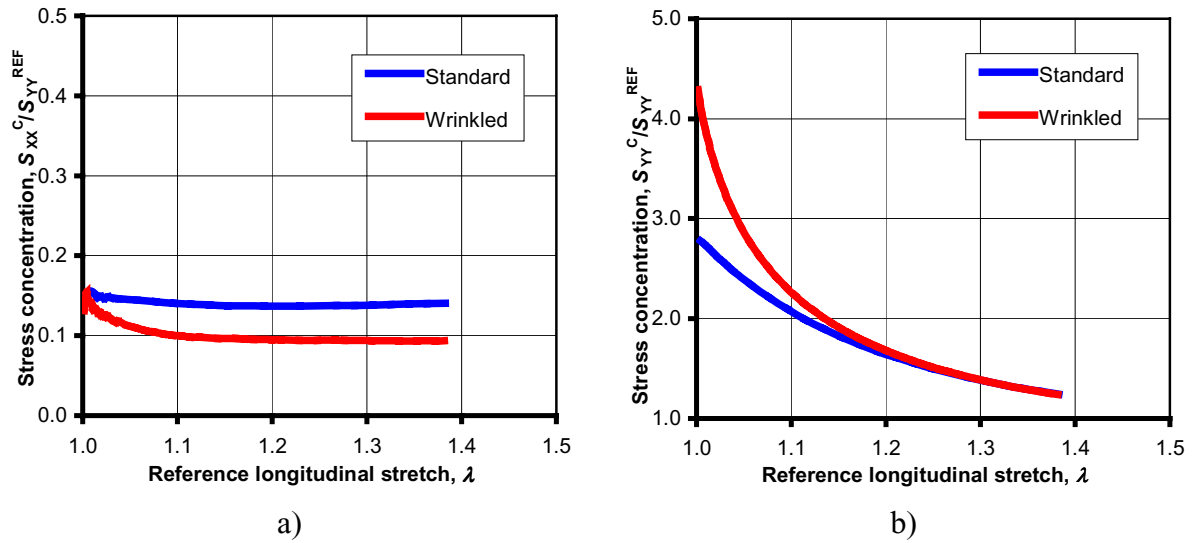


Figure 3: Rectangular membrane with a central circular hole: stress concentration.

As load is increased, the changes in the state of stress in the membrane are highlighted by the emergence of a different location of taut, wrinkled and slack regions. The evolution of the phenomenon can be valued by examining the sequence of the deformed configurations. Figure 4 shows some of these, correspondingly to the incremental steps given in Table 1.

A slack region can be observed in the neighbourhood of the hole at the very first steps. However, this region soon vanishes as the reference longitudinal stretch increases.

Incremental step	0	1	21	27	37	53
Reference stretch	1.000	1.002	1.047	1.104	1.200	1.353
Load multiplier	0.000	0.114	2.835	5.928	10.344	15.974

Table 1: Rectangular membrane with a central circular hole: incremental steps.

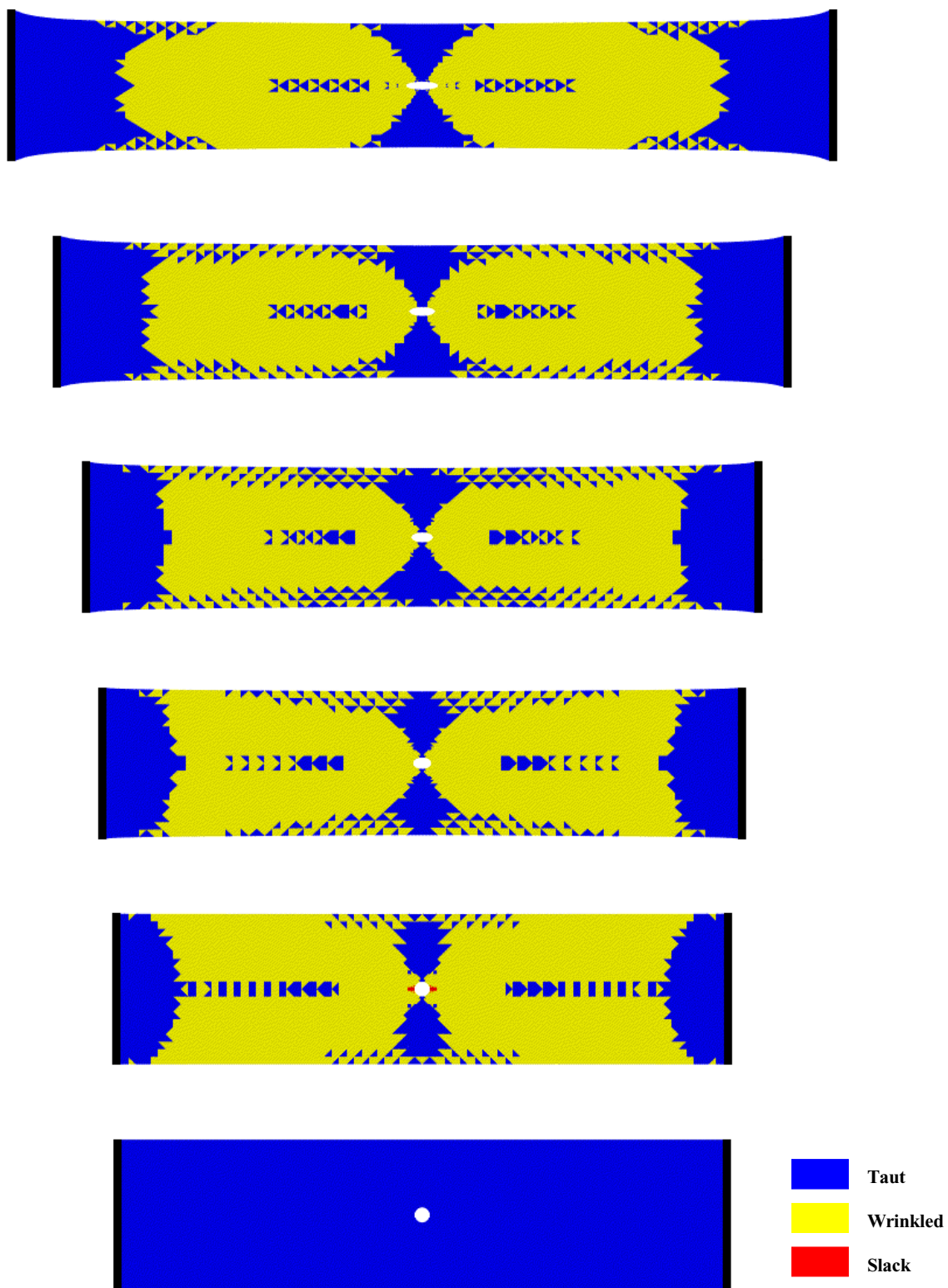


Figure 4: Rectangular membrane with a central circular hole: sequence of equilibrium configurations.

3.2 Rectangular membrane with a central circular rigid inclusion

The second application case considers the presence of a central circular rigid inclusion in the membrane. Geometry, loads and FEM model are as in the previous example (Figures 1a and 1b), except for the conditions at the internal boundary which is now fixed. Again, analysis was carried out using both the standard membrane theory and the wrinkled membrane theory.

Figure 5a represents the load multiplier, μ , as a function of the reference longitudinal stretch, λ . No appreciable discrepancy can be noticed between the two analysis cases, meaning that the global behaviour of the membrane is apparently the same. Figure 5b shows the transversal displacements of point **B** of the membrane as the load multiplier, μ , is increased. Slightly larger displacements are obtained from the wrinkled membrane theory model.

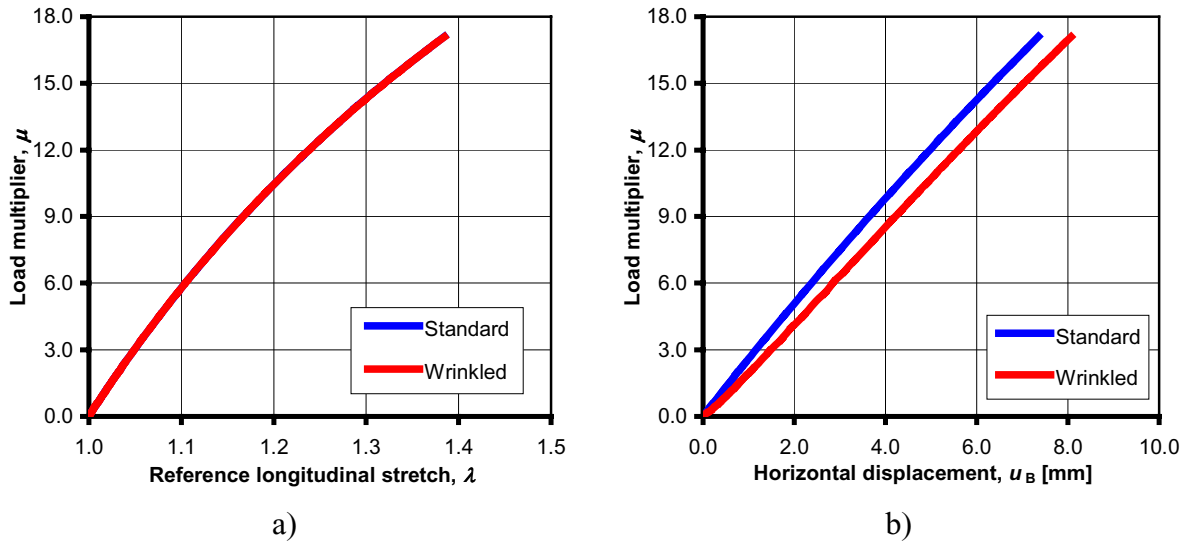


Figure 5 Rectangular membrane with a central circular rigid inclusion: equilibrium path.

Figure 6a shows the ratio, S_{XX}^C/S_{YY}^{REF} , between the S_{XX} stress component in the neighbourhood of point **C** and the reference stress, S_{YY}^{REF} , as a function of the reference longitudinal stretch, λ . Figure 6b represents the ratio, S_{YY}^C/S_{YY}^{REF} , vs. λ . Results from the two analysis cases differ qualitatively. In fact, while the standard membrane theory predicts an increasing stress concentration for both stress components, the wrinkled membrane theory furnishes a rigorously zero S_{XX} and a negligible S_{YY} .

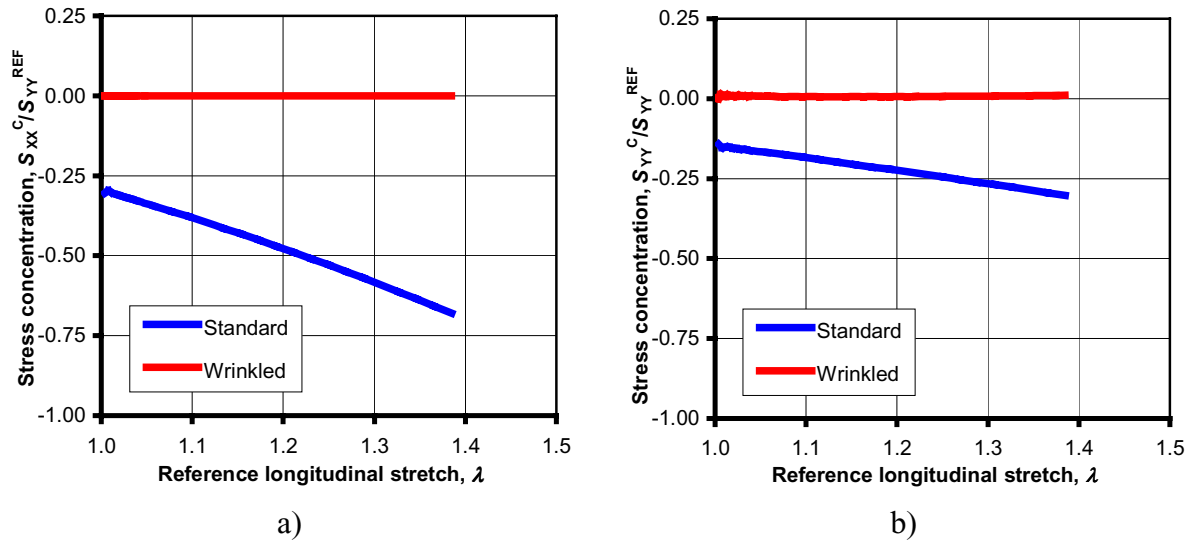


Figure 6: Rectangular membrane with a central circular rigid inclusion: stress concentration.

The surfacing of taut and wrinkled regions as load is increased, can be appreciated from Figure 7 that shows a sequence of deformed configurations of the membrane corresponding to the incremental steps given in Table 2.

Incremental step	0	1	21	27	37	53
Reference stretch	1.000	1.002	1.048	1.105	1.202	1.356
Load multiplier	0.000	0.123	2.925	6.053	10.508	16.183

Table 2: Rectangular membrane with a central circular rigid inclusion: incremental steps.

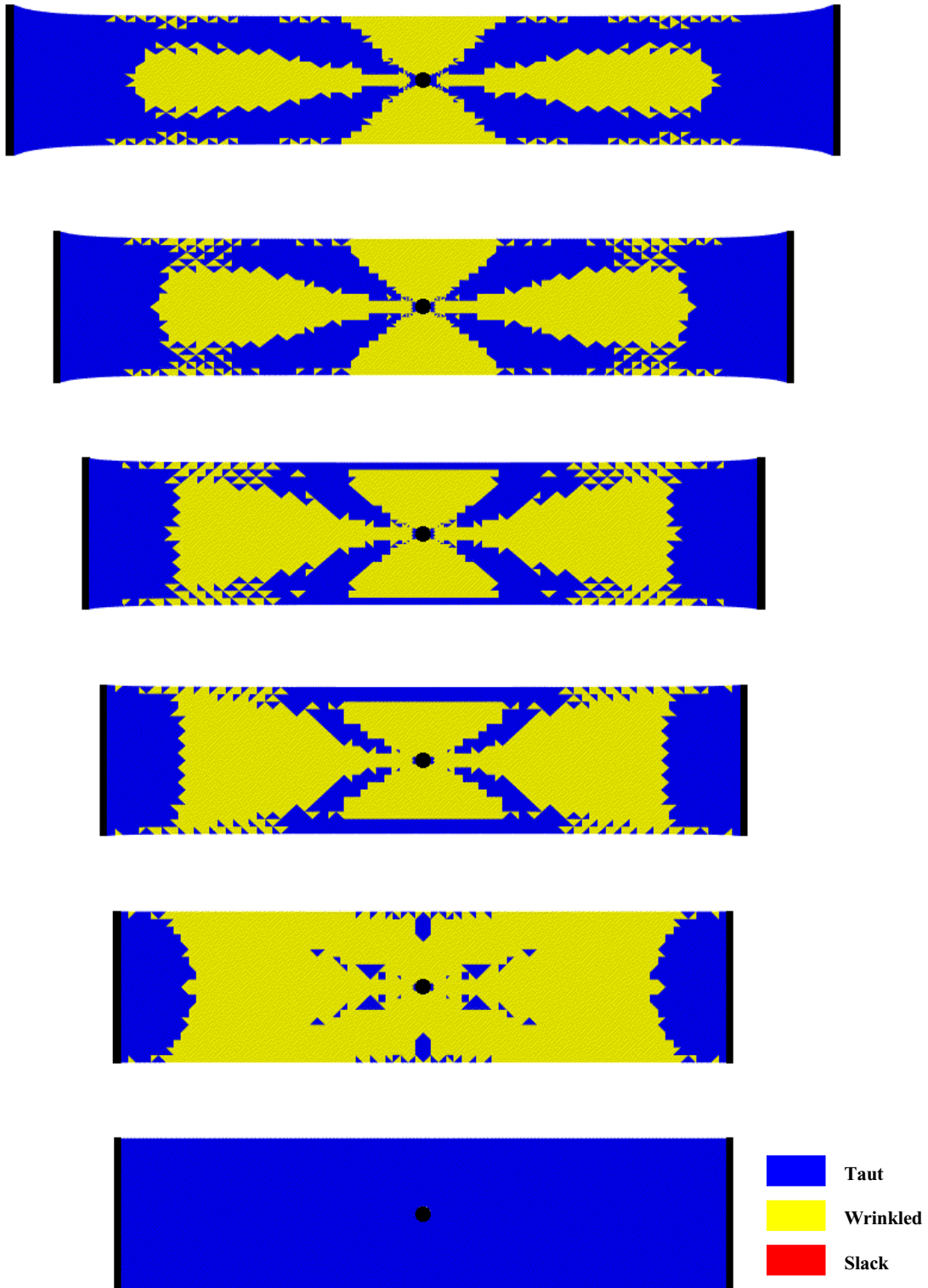


Figure 7: Rectangular membrane with a central circular rigid inclusion: sequence of equilibrium configurations.

3.3 Rectangular membrane with a central slit

In the third case presented, the membrane is endowed with a central slit (Figure 8a). Only a quarter of the membrane is considered in the FEM model. It comprises 550 nodes and 983 constant strain/constant stress triangular elements, including 20 “very stiff” elements used to enforce the rigidity constraint at the loaded edge (Figure 8b).

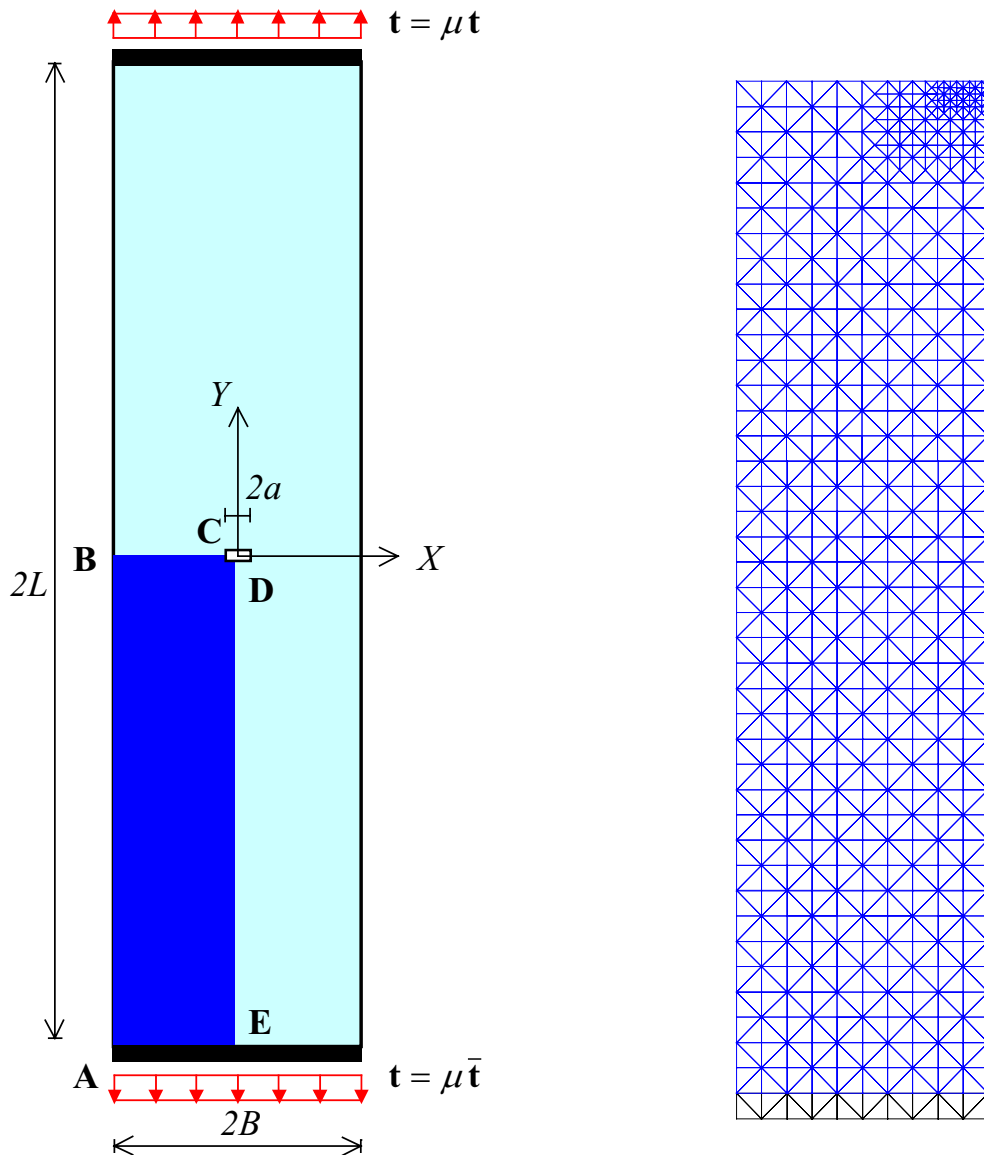


Figure 8: Rectangular membrane with a central straight defect: a) geometry and loads; b) FEM model.

Analysis was again carried out by using standard membrane theory and wrinkled membrane theory. Figure 9a represents the load multiplier, μ , in terms of the reference longitudinal stretch, λ . No appreciable discrepancy can be noticed between the two analysis cases,

meaning that the global behaviour of the membrane is still the same. Figures 9b, 9c and 9d show the transversal and longitudinal displacements of points **B**, **C** and **D** as the load multiplier, μ , is increased. Larger displacements are obtained from the wrinkled membrane theory model.

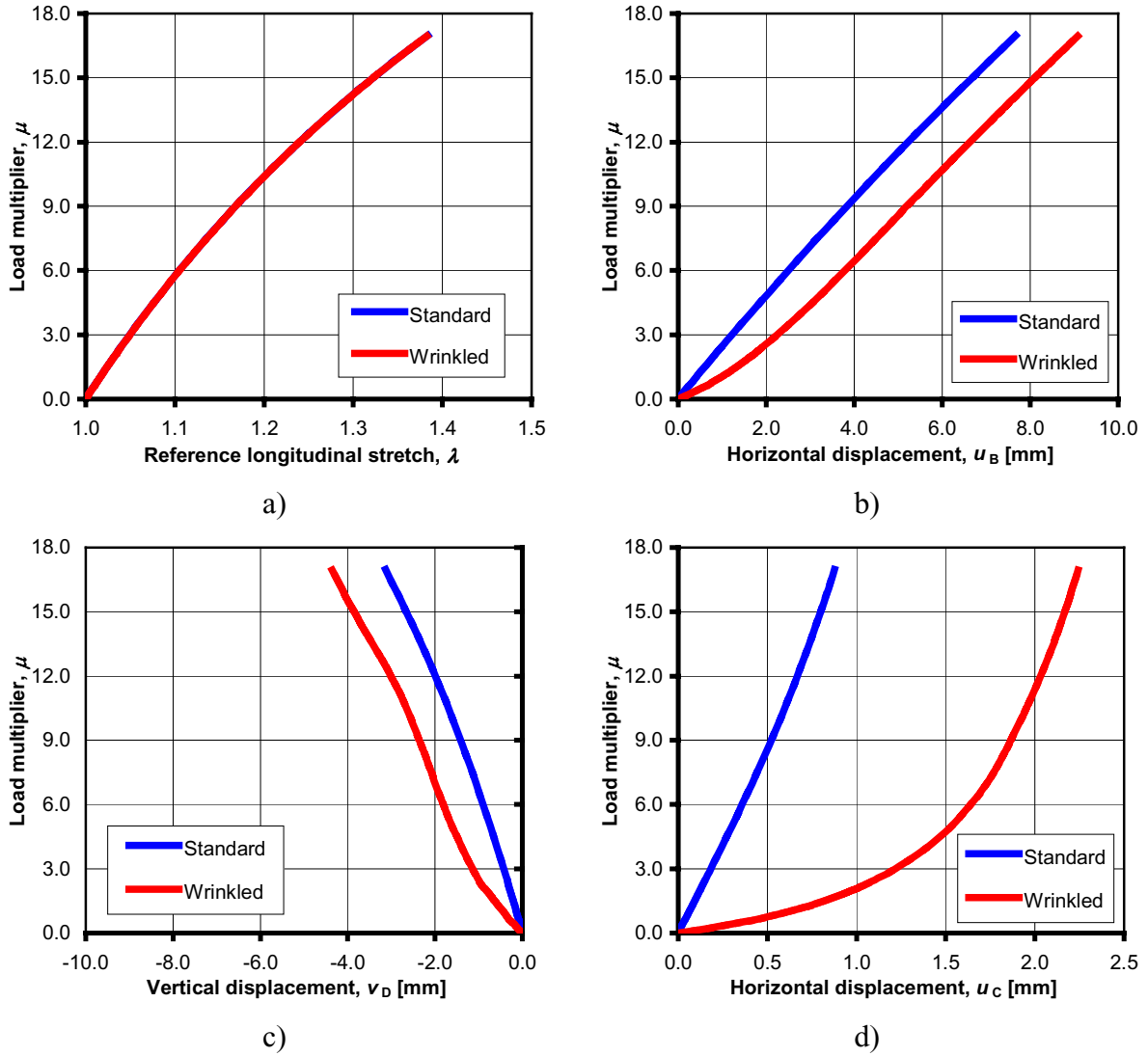


Figure 9: Rectangular membrane with a central slit: equilibrium path.

Figure 10a shows the ratio, S_{XX}^C/S_{YY}^{REF} , as a function of the reference longitudinal stretch, λ . The S_{XX} stress-concentration is less severe if wrinkling effects are considered. Figure 10b represents the ratio, S_{YY}^C/S_{YY}^{REF} , vs. λ . For this stress component, only a slight discrepancy can be noticed between the two analysis cases.

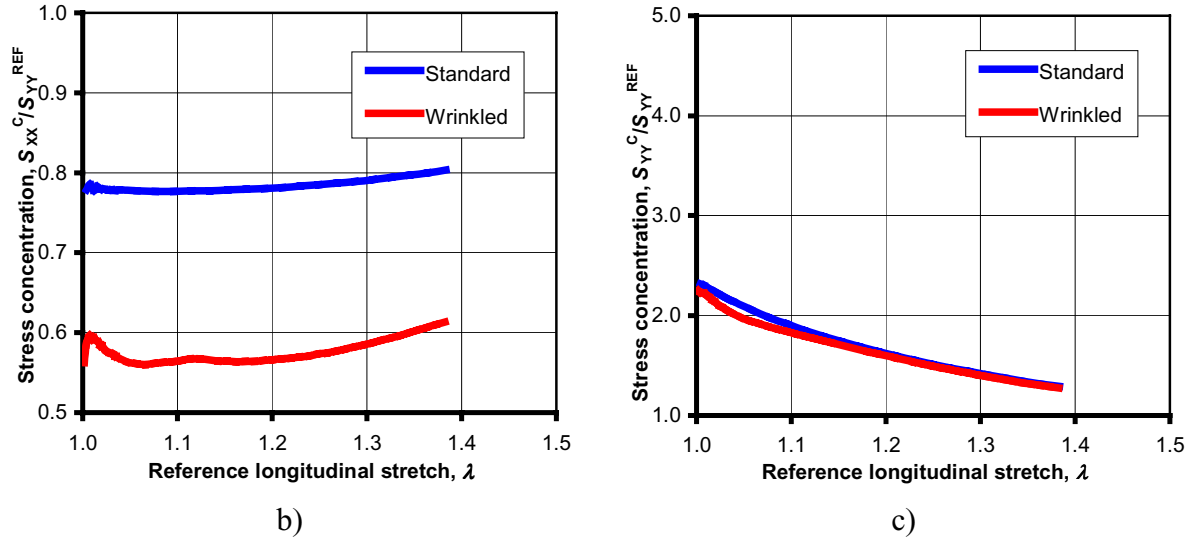


Figure 10: Rectangular membrane with a central slit: stress concentration.

As load is increased, a different location of taut, wrinkled and slack regions appears on the membrane surface. Figure 11 shows the deformed configurations corresponding to the incremental steps given in Table 3. A slack region is clearly observable in the neighbourhood of the slit at all the steps considered.

Incremental step	0	1	21	27	37	53
Reference stretch	1.000	1.002	1.047	1.104	1.200	1.354
Load multiplier	0.000	0.116	2.855	5.960	10.391	16.040

Table 3: Rectangular membrane with a central slit: incremental steps.

3.4 Rectangular membrane with a central straight rigid inclusion

The last application case concerns the presence of a central straight rigid inclusion. Geometry, loads and FEM model are as in the previous example (Figures 8a and 8b), except for the conditions at the internal boundary which is now fixed. Again, analysis was carried out using both the standard membrane theory and the wrinkled membrane theory.

Figure 12a represents the load multiplier, μ , in terms of the reference longitudinal stretch, λ . No appreciable discrepancy is found between the two analysis cases. Figure 12b shows the transversal displacements of point **B** as μ is increased. Slightly larger displacements are predicted by the wrinkled membrane theory.

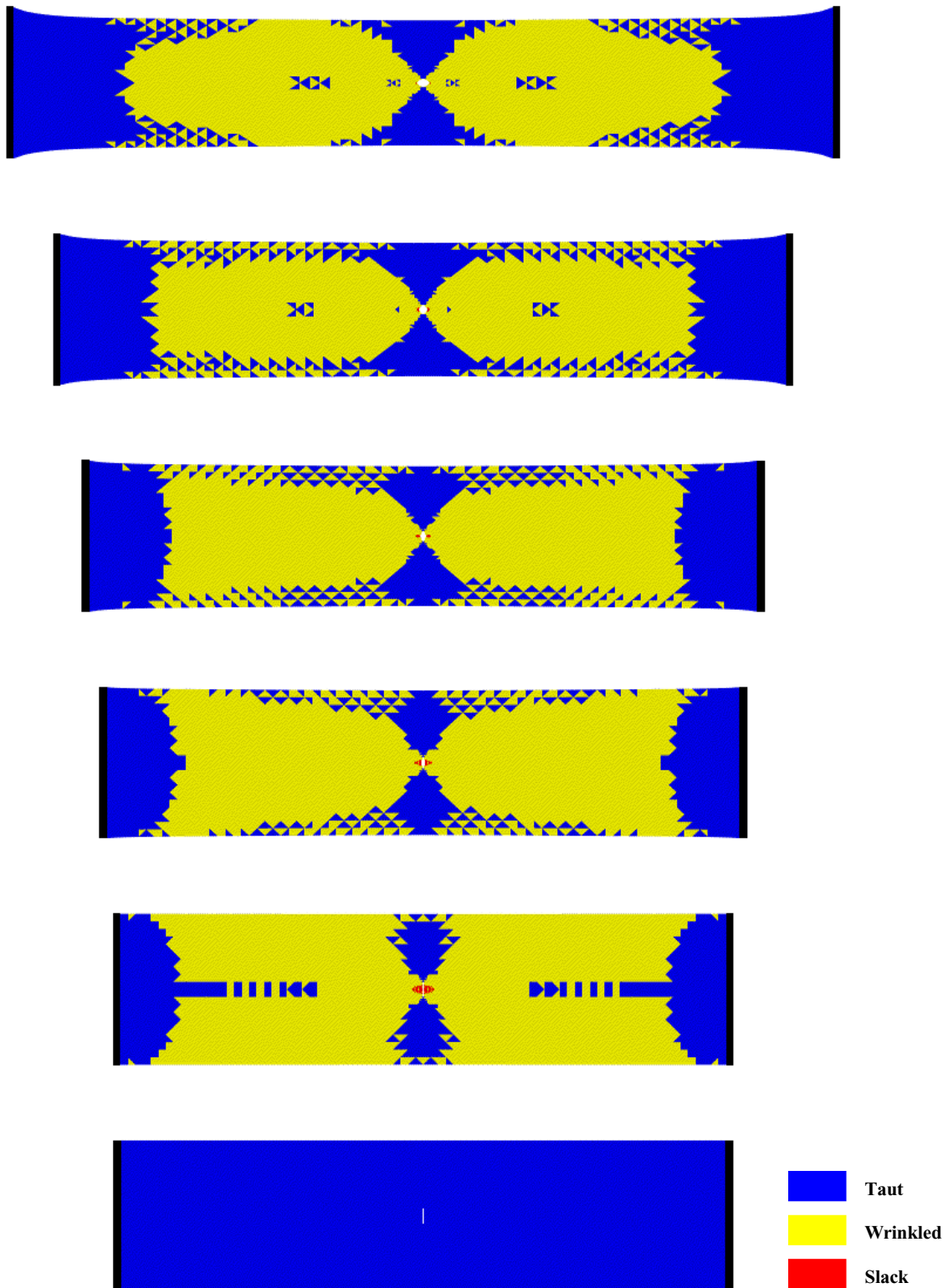


Figure 11: Rectangular membrane with a central slit: sequence of equilibrium configurations.

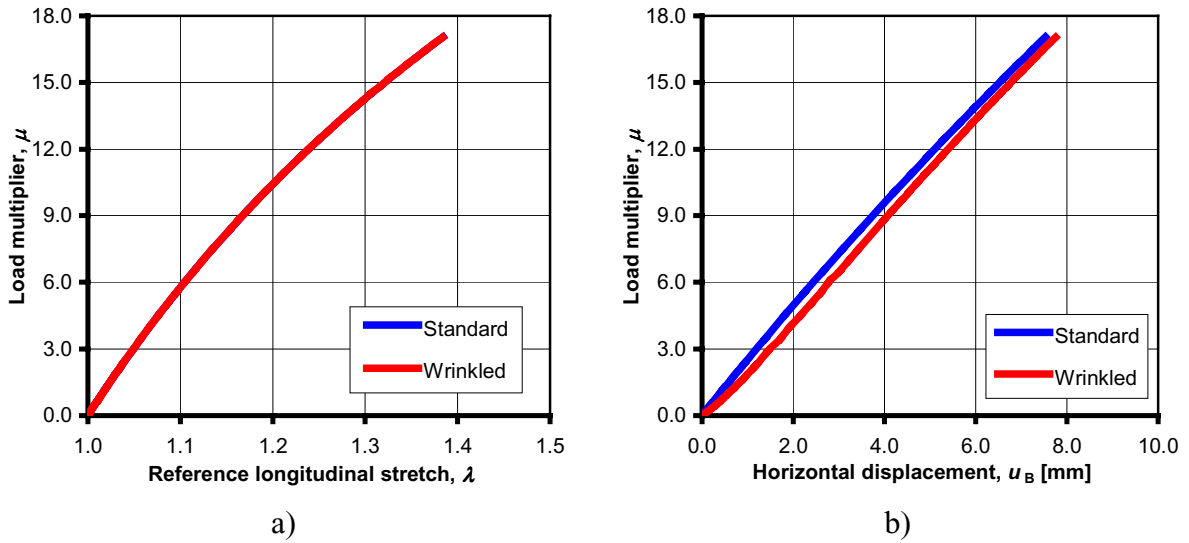


Figure 12: Rectangular membrane with a central straight rigid inclusion: equilibrium path.

Figure 13a shows the ratio, S_{XX}^C/S_{YY}^{REF} , in terms of the reference longitudinal stretch, λ . Predictions of the wrinkled membrane theory are less severe, since this stress component assumes nearly negligible values. Figure 13b represents the ratio, S_{YY}^C/S_{YY}^{REF} , as a function of λ . For this stress component, it is the standard membrane theory that gives less severe predictions.

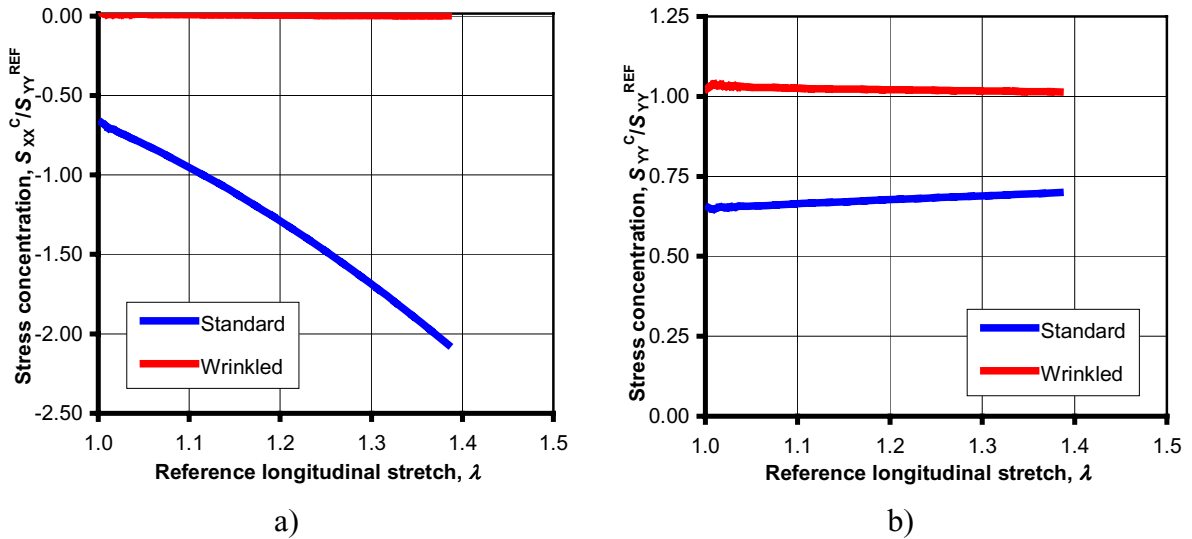


Figure 13: Rectangular membrane with a central straight rigid inclusion: stress concentration.

Figure 14 shows the deformed configurations at the incremental steps given in Table 4.

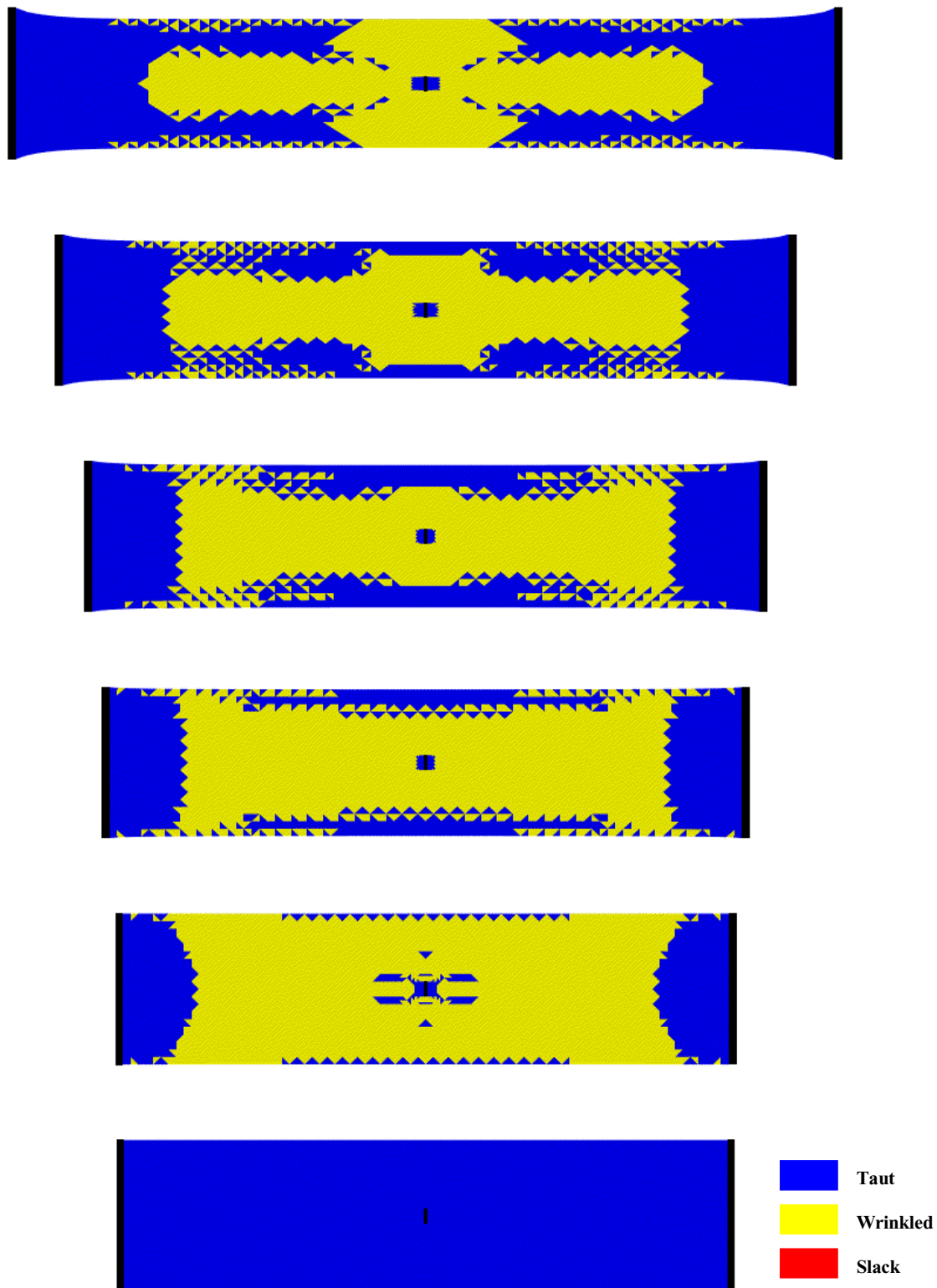


Figure 14: Rectangular membrane with a central straight rigid inclusion: sequence of equilibrium configurations.

Incremental step	0	1	21	27	37	53
Reference stretch	1.000	1.002	1.048	1.105	1.201	1.355
Load multiplier	0.000	0.122	2.915	6.035	10.477	16.135

Table 4: Rectangular membrane with a central straight rigid inclusion: incremental steps.

4 Conclusions

A model was presented for determining the stress distribution around discontinuities, such as holes or rigid inclusions, in soft elastic membranes subjected to increasing loads. Characterising issues are:

- a) the adoption of a non-linear material law suitable for large deformations;
- b) the possibility of automatic account for local buckling and wrinkling phenomena;
- c) the implementation of the mechanical model within a FEM framework, where a wide variety of problems can be further posed and solved;
- d) the use of an incremental-iterative strategy that permits to monitor the evolutionary aspects.

Applications, concerning a rectangular membrane endowed with a central circular or straight defect, showed that the stress concentration is always very different from that predicted by Linear Elastic Fracture Mechanics and can be in some cases less severe.

References

- [1] G. A. Holzapfel, *et al.*, *Large strain analysis of soft biological membranes: Formulation and finite element analysis*, Comput. Meths. Appl. Mech. Engrg., 132, (1996), 45-61.
- [2] J. Shi, G. F. Moita, *The post-critical analysis of axisymmetric hyper-elastic membranes by the finite element method*, Comput. Meths. Appl. Mech. Engrg., 135, (1996), 265-281.
- [3] C. H. Wu, *Nonlinear wrinkling of nonlinear membranes of revolution*, J. Appl. Mech., 45, (1978), 533-538.
- [4] R. W. Ogden, *Non-linear elastic deformations*, Ellis-Horwood, Chichester, (1984).
- [5] A. C. Pipkin, *The relaxed energy density for isotropic elastic membranes*, IMA J. Appl. Math., 36, (1986), 85-99.
- [6] D. J. Steigmann, A. C. Pipkin, *Wrinkling of pressurized membranes*, J. Appl. Mech., 56, (1989), 624-628.
- [7] M. A. Crisfield, *A fast incremental/iterative solution procedure that handles snap-through*, Computers & Structures, 13, (1981), 55-62.